www.czasopisma.pan.pl PAN www.journals.pan.pl

Opto-Electronics Review 25 (2017) 198–204

Contents lists available at ScienceDirect

Opto-Electronics Review

journal homepage: http://www.journals.elsevier.com/opto-electronics review

Influence of the core size on light propagation in photonic liquid crystal fibers

M.M. Sala-Tefelska [a,*], S. Ertman [a], T.R. Woliński [a], P. Mergo [b]

[a] Faculty of Physics, Warsaw University of Technology, Koszykowa 75, 00-662 Warsaw, Poland
[b] Maria Sklodowska-Curie University, Pl. Marii Curie-Skłodowskiej 3/607, 20-031 Lublin, Poland

ARTICLE INFO

Article history:
Received 22 January 2017
Received in revised form 15 June 2017
Accepted 27 June 2017
Available online 24 July 2017

Keywords:
Photonic liquid crystal fibers
Attenuation
Confinement losses
Modes

ABSTRACT

In this paper analyses of mode distribution, confinement and experimental losses of the photonic crystal fibers with different core sizes infiltrated with liquid crystal are presented. Four types of fibers are compared: with single-, seven-, nineteen- and thirty seven solid rods forming the core in the same hexagonal lattice of seven "rings" of unit cells (rods or capillaries). The experimental results confirming the influence of the core diameter on light propagation are also included. The diameter of cores determines not only the number of modes in the photonic liquid crystal fiber but also is correlated with experimentally observed attenuation. For fibers with larger cores confinement losses are expected to be higher, but the measured attenuation is smaller because the impact of liquid crystal material losses and scattering is smaller.

1. Introduction

Photonic crystal fibers (PCF) are two-dimensional structures made of silica glass with a periodically distributed refractive index. They consist of micro-holes which are surrounding a solid or hollow core [1–4]. Light propagation within such a structure depends on the ratio between the refractive index of the fiber core and the mean refractive index of the cladding. When the solid core is characterized by a higher refractive index than the index of a photonic crystal cladding, light is guided by the mechanism called modified total internal reflection (mTIR) also known as index guiding. When the refractive index of the solid core is lower than the cladding index, the photonic band gap (PBG) mechanism of light propagation is obtained. For the last years many different types of photonic crystal fibers, both hollow-core and solid-core have been demonstrated [5–7]. PCFs filled with liquid crystals (LCs) have a great number of potential applications in a new class of in-fiber devices such as polarization controllers, tunable filters or optical filters [8–11] whereas liquid crystals as anisotropic materials offer unusual optical properties (such as, e.g. tunable birefringence, optical activity, selective Bragg reflection, circular dichroism) that can be easily modified by external physical fields [12].

One of the serious issues related with any optical fiber and in particular with a PCF is attenuation, which is usually determined by absorption and material scattering (heterogeneity of the structure and spatial distribution of the refractive index) but also by a number of connectors or splices [13]. PCFs made of pure silica glass can have attenuation less than 0.48 dB/km at 1550 nm [14,15]. To increase the refractive index of the solid-core PCF, silica glass is doped with either erbium or germanium. Unlikely, attenuation of such a structure is higher up to 0.97 dB/km at the wavelength of 1.55 μm [16,17]. Moreover, not only doping but also modifications in the photonic structure, as well as infiltration of the air holes with different materials (as e.g. with LCs that scatter light strongly) may significantly increase fiber losses.

Despite of this, liquid crystals due to their very interesting anisotropic properties have been successfully used in the so-called photonic liquid crystal fibers (PLCFs), i.e. PCFs filled with liquid crystals [18–21]. It has been already showed that guiding properties of the PLCFs can be easily modified by an external electric field or by temperature. There are two important parameters that influence the light propagation in PLCFs, i.e. the core size and the scattering properties of the LC [22,23]. Scattering losses can be reduced by using a low birefringence LC [24]. In other works concerning PLCF, not only the attenuation properties, but also the waveguide dispersion can be elegantly tuned [25–27].

The aim of this study is to show that a change in the diameter of the fiber core can modify not only confinement losses of the PLCF, but also the amount of the optical power that is guided in strongly scattering LC-filled holes, by studying four fibers with a drastically varying core diameter. It is expected that fiber attenuation is smaller if propagation through the LC-filled holes is lower.

* Corresponding author.
E-mail address: martef@if.pw.edu.pl (M.M. Sala-Tefelska).

http://dx.doi.org/10.1016/j.opelre.2017.06.013
1896-3757/

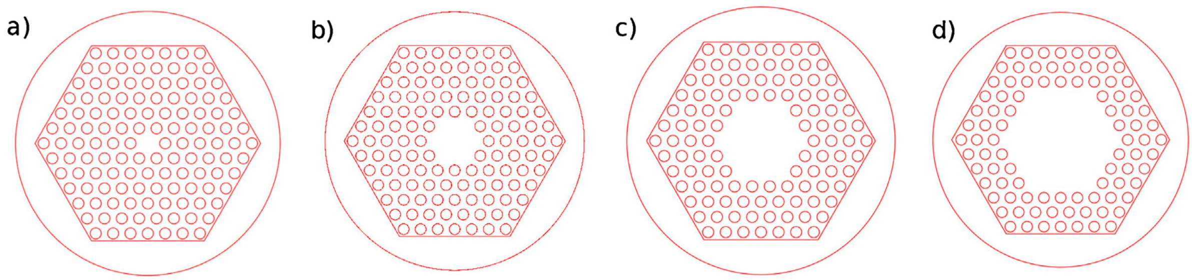

Fig. 1. Structures of the photonic crystal fibers. The core consists of (a) 1 rod (PCF 1), (b) 7 rods (PCF 7), (c) 19 rods (PCF 19), (d) 37 rods (PCF 37).

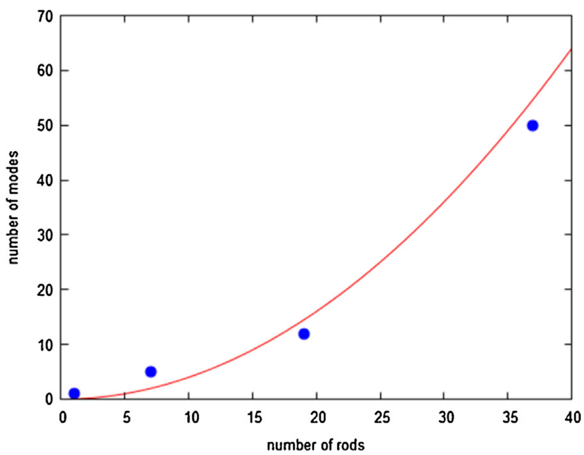

Fig. 2. Number of modes *vs.* number of rods forming the fiber core with quadratic fitting (red solid line).

Interesting results were reported in Ref. [28] where a PLCF with a very large core had a very low attenuation in the PBG mechanism compared to a similar structure with a single-defect core. In this work analyses of mode distribution, confinement and experimental losses for different fiber core diameters and also experimental results with designed fibers are presented.

The paper is organized as follows: in Section 2 fibers' parameters, theoretical analysis of four types of PCF structures infiltrated with LC are presented and in Section 3 experimental results obtained are compared with the theory.

2. Numerical simulation

Structures of different PCFs under consideration are presented in Fig. 1. All the structures are based on a similar lattice consisting of seven rings of solid rods or capillaries, with the lattice constant $\Lambda = 8.4\,\mu m$ and the diameter of the holes $d = 5.7\,\mu m$. The first one is a typical fiber with the core consisting of a single rod (named PCF 1) surrounded by six rings of holes. The second one has the core consisting of 7 rods (named PCF 7) surrounded by 5 rings of holes. The third one has the core consisting of 19 rods (named PCF 19) surrounded by 4 rings of holes. The last one has 37 rods (named PCF 37) surrounded by 3 rings of holes. The PCF1 is a single mode fiber, while PCFs 7, 19 and 37 are multimode photonic crystal fibers.

The PCF structures and fiber modes were analyzed by using the commercially available software Comsol 3.5a which is based on a fully vectorial finite-element algorithm [29,30]. Simulations were performed for the wavelengths within the range of 200 ÷ 850 nm. Liquid crystal dispersion was not taken into account, whereas dielectric anisotropy was represented by the diagonal tensor of dielectric permittivity $\varepsilon_{xx} = \varepsilon_{yy} = 1.4614$, $\varepsilon_{zz} = 1.5225$ (planar orientation was assumed) at 25 °C, characterizing the 1550 nematic liquid crystal mixture used in the experiment [31,32]. The PCF structure was represented by the refractive index of the fused silica determined from the Sellmeier equation and it is equal to 1.45 at 0.6 µm [33]. A typical mode field area of the fundamental mode for PCF37 core is ~2525 μm^2, for PCF19 is ~1140 μm^2, PCF7 is 411 μm^2 and PCF1 is 74 μm^2.

The PCF37, PCF19, and PCF7 are multimode fibers in both cases when the holes are either empty or filled with liquid crystal. For example, for the empty PCF 37 it was possible to find more than 100 modes. For the fibers filled with the LC, multimode photonic bandgap propagation has been obtained numerically. In the following part of the paper the PLCFs stand for photonic crystal fibers infiltrated with liquid crystals (i.e. PLCF1, PLCF7, PLCF19, and PLCF37).

For PLCF37 it was usually more than 50 modes (which were thoroughly analyzed), for PLCF19 it was about 12 modes, for PLCF7 it was 5 modes. PLCF 1 guides only a single mode but for particular wavelengths (e.g. $\lambda = 645$ nm) second mode was observed with high losses. It is worth to mention that the position of the PBGs is determined by properties of the cladding holes infiltrated with the LCs. The higher order modes are guided in the same range of wavelengths as the fundamental mode. The criterion of the modes number results from the observation of modes' profiles depending on the wavelength, until the moment when cladding modes appear, (i.e. when the power of light propagating in the holes filled with LCs, expressed as a percentage of the total power, is higher than

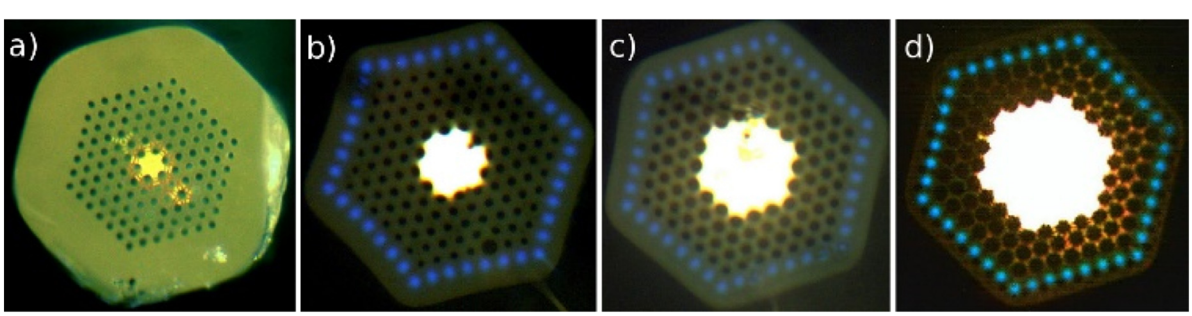

Fig. 3. Microscope images of the cross-section of empty photonic crystal fibers with different cores. (a) PCF1 (b) PCF7, (c) PCF19, (d) PCF37, (The mTIR mechanism of light propagation in fibers is observed).

Table 1
The percentage of optical power guided through the LC-filled sections (at 620 nm) for I PBG.

	Fund. mode	2^{nd} mode	3^{rd} mode	5^{th} mode	7^{th} mode
PLCF 37	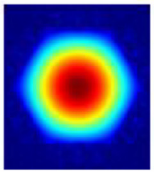	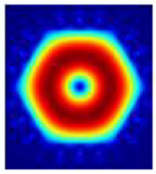	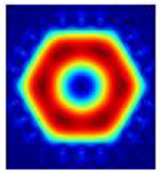	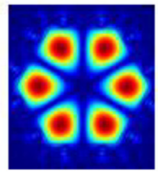	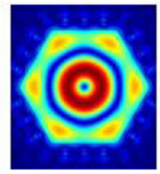
%	0.07%	0.20%	0.37%	0.60%	0.76%
PLCF 19	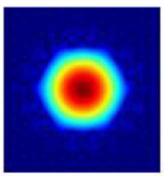	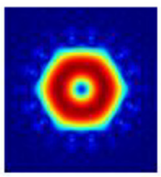	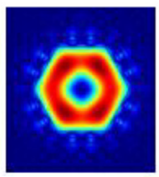	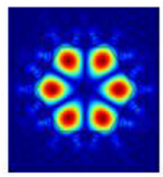	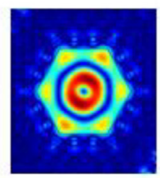
%	0.17%	0.50%	0.99%	1.91%	2.40%
PLCF 7	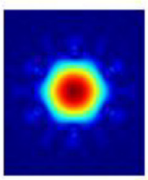	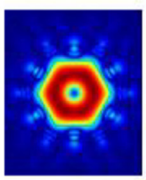	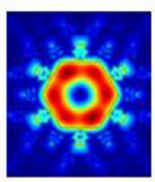	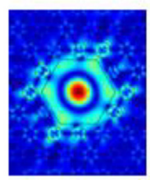	
%	0.75%	2.48%	8.97%	4^{th} mode 26.50%	
PLCF 1	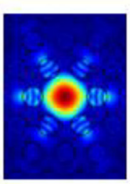				
%	12.00%				

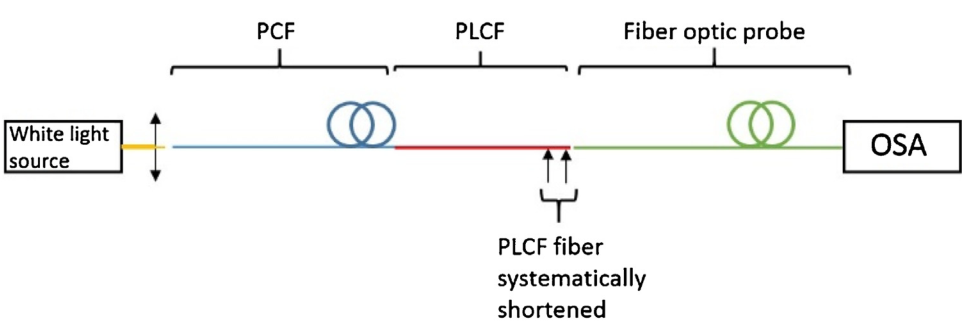

Fig. 4. Experimental setup.

10%), see Table 3 [21]). The collected data indicate that the number of modes increases with the number of rods as it is presented in Fig. 2. PCF37 (Fig. 1d) is a "truly" multi-mode fiber with a high number of well-guided band-gap modes. Changes in the d/Λ ratio can lead to propagation of few higher-order modes in an empty fiber and especially in single-defect PCFs. In PCF37 this situation is slightly different since core dimensions are much larger than the guided wavelength and even in the case of the d/Λ ratio smaller

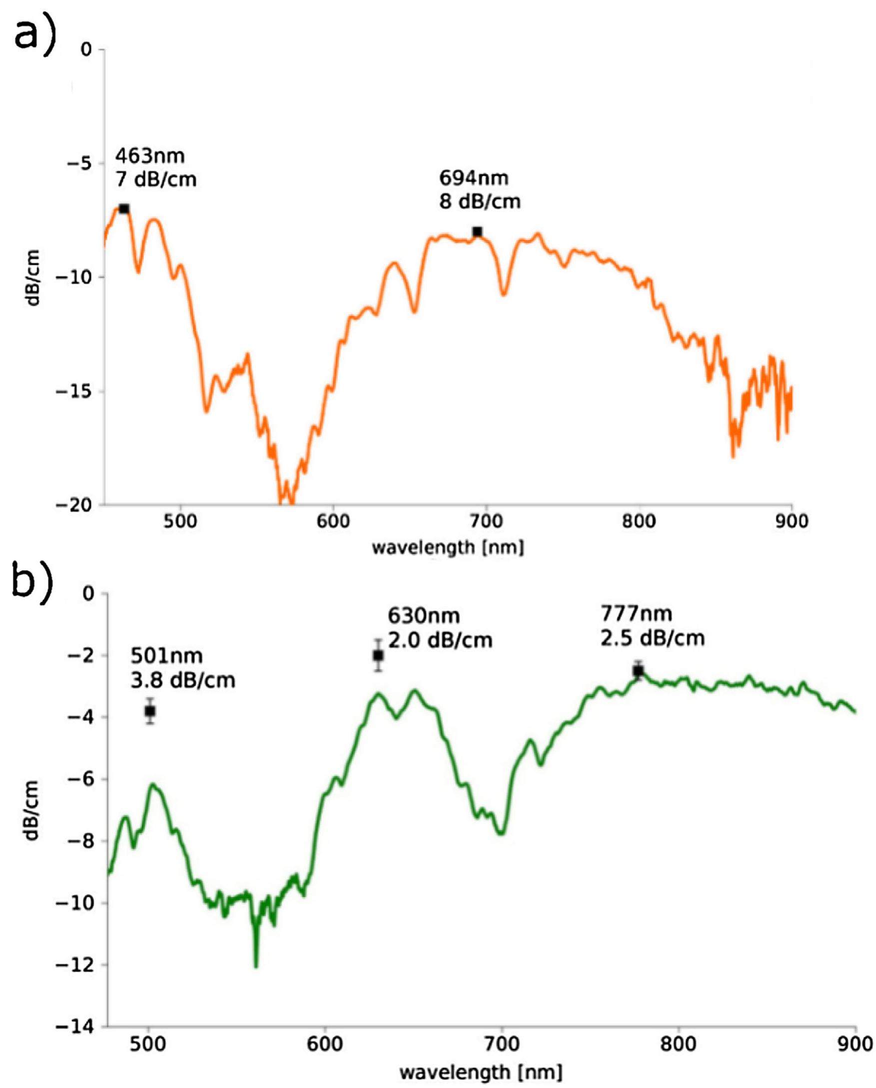

Fig. 5. Single attenuation measurement for: (a) 3 cm of the PLCF1 at 23 °C (orange solid line), (b) 9 cm of the PLCF7 at 23 °C (green solid line). Black crosses represent the attenuation measured by the cut-back technique (see also Ref. [35]).

than 0.4 [2] it is possible to obtain multimode propagation. However, in this case the d/Λ ratio was rather determined by expected properties of the photonic band gap of the cladding after infiltration with the 1550 low-birefringence liquid crystal mixture [31,32]. Since the propagating wavelengths are determined by the photonic bandgaps formed in the cladding and due to a large diameter of the core it is possible to obtain a high number (>50) of spatial modes for each of the guided wavelengths. Our calculations show that in large-core fibers less than 1% of the optical power is guided through the sections filled with a liquid crystal, since in the "single-defect" PLCFs ~10–20% of the optical power is guided through the sections filled with a liquid crystal. In Table 1 percentage of the optical power penetrating into the holes is presented for the first PBG at 620 nm for selected modes of all four analyzed PLCF structures. Light penetration in the holes for the first PBG of PLCF 37 is very low and it increases with higher-order modes.

In PLCF 19 optical power of the fundamental mode penetrating into the holes is higher than for PLCF37. It is the same for PLCF 7 and for PLCF1 where the optical power in the air holes is very high. The explanation of this phenomena is quite intuitive – in the case of photonic band-gap propagation the mode profile in the microstructured cladding is very similar for both higher-order modes and the modes calculated for the fibers with various core sizes. If the fiber's core size is increasing simultaneously, the amount of optical power guided in the core is increasing and a smaller percentage of total optical power is penetrating the cladding.

Table 2
The percentage of optical power penetrating holes of the PLCF 37.

PBG	Fundamental mode [%]
I	0.07
II	0.32
III	0.06

It can be also noticed that the percentage of optical power guided through the LC holes varies for higher order modes. Due to the fact that a number of modes than can be propagated in each PBG (all the fibers are multimode), attenuation observed experimentally would be somehow "averaged" from a large number of possible modes.

Table 1 presents the results obtained for one selected PBG (first order – I PBG), but similar phenomena were observed for other bandgaps. However, it appeared that the percentage of the optical power penetrating LC holes varies for different PBGs (example for PLCF37 is presented in Table 2). It may explain why some of the photonic band gaps of real PCFs have lower attenuation than others. On the other hand, a real PCF structure is neither perfectly uniform nor symmetrical and it is possible that some PBGs are more sensitive for these deviations in the PCF structure.

3. Experimental results

The confinement losses [34] calculated theoretically are much lower than the losses observed in the experiment, so this phenomenon rather relates to physical properties of the fiber which were not included in the numerical model (i.e. scattering by the LC, fluctuations of the holes size, their shape, and position in PCF structure).

The number of rings in the PCF structure introduces changes in the confinement losses of the guided modes (both index-guided and PBG modes). Theoretically, it is possible to reduce confinement losses to a very low value by adding additional rings to the PCF structure. Actually, real attenuation of PLCF is determined by material losses of the LC-filled holes.

In the experiment, the size of the air-holes is slightly different (Fig. 3). The real parameters of fabricated PCFs are presented below. The experimental setup consists of NKT Photonics SuperK Compact Supercontinuum White Light laser as a light source with a broadband output spectrum covering the 500–2400 nm range. The total average output power is above 100 mW. The Ocean Optics HR4000 spectrometer with a 0.2-nm optical resolution and the Optical Spectrum Analyzer Ando (wavelength range from 350 to 1750 nm) were used as detectors.

The used photonic crystal fibers were fabricated at Maria Sklodowska-Curie University (Lublin, Poland). The rods and capillaries were made of Heralux WG silica glass. The manufactured fibers are characterized by the following parameters: the PCF1 has 4.1 μm diameter of holes and lattice constant 6.5 μm (Fig. 5a); the PCF7 has 4.7 μm diameter of holes and lattice constant 9.6 μm (Fig. 5b); the PCF19 has 4.8 μm diameter of holes and lattice constant 9.4 μm (Fig. 5c); the PCF37 has 5.7 μm diameter of holes and lattice constant 8.4 um (Fig. 5d). The last PCF is characterized by a very large core diameter.

The PCFs were filled with a 1550 low-birefringence nematic LC mixture (synthesized at the Military University of Technology, Warsaw, Poland) [31,32]. The PBG propagation was observed. The 1550 LC is characterized by anisotropy $\Delta n = 0.06$, where $n_e = 1.52$, $n_o = 1.46$, at T = 25 °C. Hence, fiber attenuation was measured only at the wavelengths at which PBGs appear. The flow of the LC during the infiltration process generally induces planar orientation of the LC molecules within the micro-holes. To measure attenuation of the PLCFs, the cut-back technique was applied, i.e. the PLCF length was being systematically shortened and the spectrum of a PLCF was analyzed. The experimental setup is presented in Fig. 4. The lowest attenuation for PBG propagation was measured for PLCF37 (which is characterized by a very large core) and it was 0.16 dB/cm at 727 nm. The attenuation for PLCF37 is presented in Fig. 6(b). Light propagation in such a large mode field area slightly penetrates into the surrounding holes and therefore there are lower losses. The largest attenuation was measured for PBG propagation in PLCF1 which was 7 dB/cm at 463 nm [Fig. 5(a)]. For PLCF7 it was 2 dB/cm at 630 nm [Fig. 5(b)] and for PLCF19 it was 0.5 dB/cm at 808 nm [Fig. 6(a)]. It appears that a decrease of core diameter increases attenuation of the PCF infiltrated with a strongly scattering LC mixture. Selective light propagation occurs in the studied PLCFs for different liquid crystal infiltration lengths. The research shows that for a larger core, the fiber has to be filled with a liquid crystal on a longer distance to observe selective light propagation guided by the photonic band gap mechanism. On the other hand, for small core sizes attenuation is much higher so the fiber has to be filled on a shorter distance, to obtain better results.

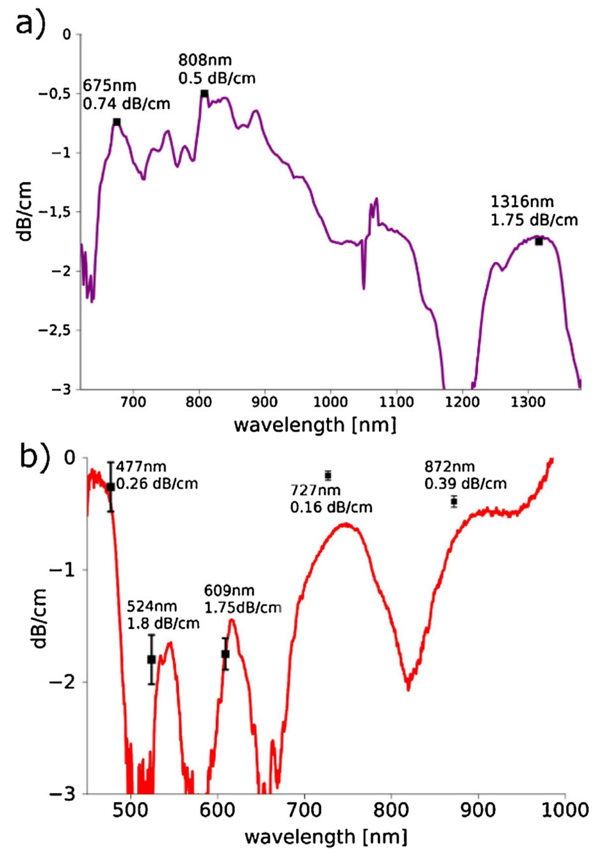

Fig. 6. Single attenuation measurement for: (a) 16 cm of the PLCF19 at 23 °C (violet solid line), (b) 23 cm of the PLCF37 at 24 °C (red solid line). Black crosses represent the attenuation measured by the cut-back technique (see also Ref. [35]).

Table 3 from left to right presents four columns of data which were numerically solved and the fifth column which shows results obtained in the experiment. The first and third columns present cladding modes with very high percentage of optical power guided through the LC holes. This is a criterion of observation of PBGs' position (the beginning and the end). The second column presents fundamental modal field distribution for a PLCF with a core consisting of 1, 7, 19, and 37 rods. In the PLCF with the largest core (PLCF 37) the propagated light slightly penetrates into the holes. This is confirmed by the sub-row below images, which shows the percentage of optical power guided through the LC-filled sections. The fourth column shows the confinement losses for PLCFs resulting from photonic crystal fiber structure – the number of holes rings. For large cores (PLCF 7, 19 and 37) the influence of core diameter on confinement losses is negligible. With an increasing number of the rings of holes the confinement losses are decreasing. However, for a PLCF with the smallest core (PLCF 1) and a large number of the rings of holes, the confinement losses are increasing. This is due to the fact that the core is very small, and the fundamental mode is "squeezed" by the photonic structure (see the second column). The fifth column refers to the experimental designation of PLCF attenuation. It was observed that the attenuation of photonic band gaps decreases with increasing dimensions of the fiber core. This is confirmed by the data obtained in simulations, see the second column. In the experiment, the confinement losses do not significantly influence light propagation in PLCFs. The largest impact on attenuation originates from light scattering and absorption of a liquid crystal. The modes that appear for the I PBG in PLCF 1, 7, 19 and 37 have almost the same range of wavelengths and it is about 130 nm (Fig. 7).

Table 3
Optical power, confinement losses and attenuation obtained in PLCFs (I PBG).

	Fundamental mode and optical power guided through the LC-filled sections			Confinement losses [dB/m]	Attenuation [dB/m]
PLCF 1 6 rings of holes	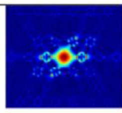	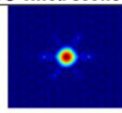	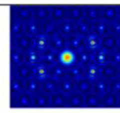	$1.5*10^{-2}$ (700nm)	$8*10^{-2}$ (at 694nm)
	612nm 42%	620nm 12.00%	720nm 55%		
PLCF 7 5 rings of holes	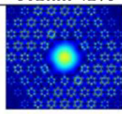	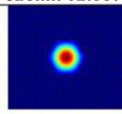	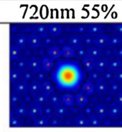	$4.8*10^{-5}$ (630nm)	$2*10^{-2}$ (at 630nm)
	600nm 50%	620nm 0.74%	726nm 50%		
PLCF 19 4 rings of holes	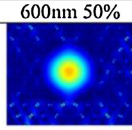	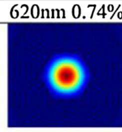	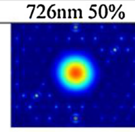	$0.8*10^{-2}$ (680nm)	$7.4*10^{-3}$ (at 675nm)
	561nm 21%	620nm 0.17%	716nm 23%		
PLCF 37 3 rings of holes	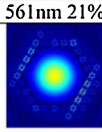	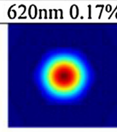	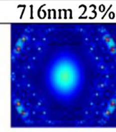	$13*10^{0}$ (730nm)	$1.6*10^{-3}$ (at 727nm)
	597nm 18%	620nm 0.07%	727nm 31%		

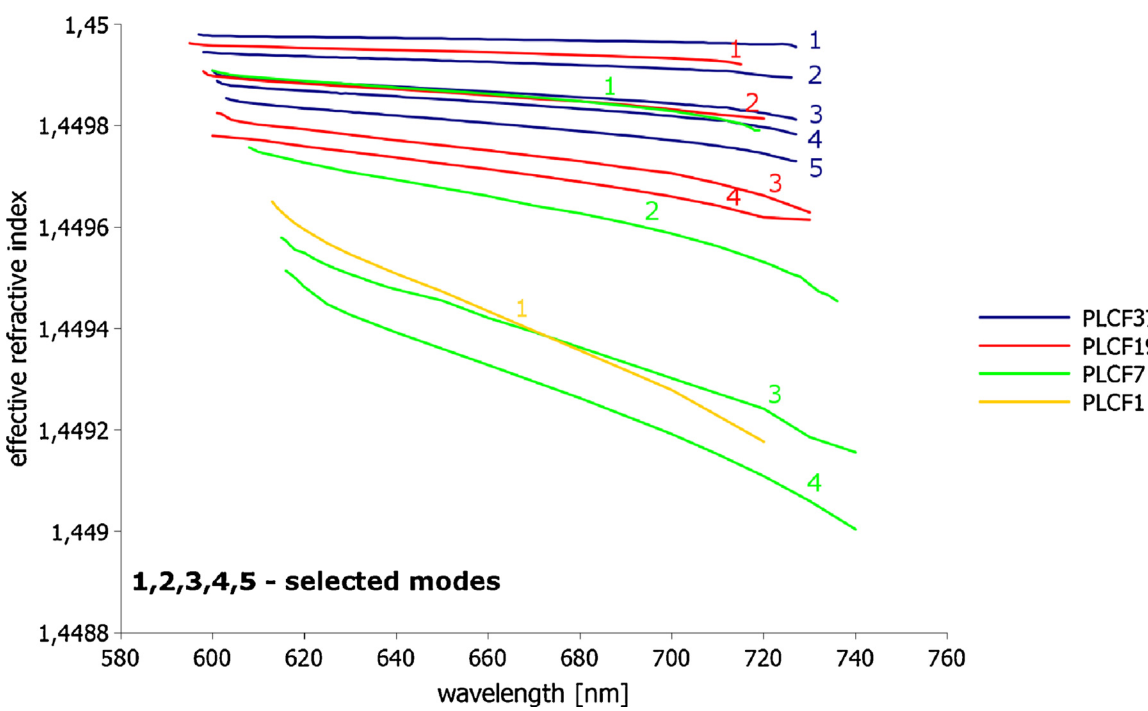

Fig. 7. The wavelength dependence of effective refractive index of selected modes for PLCF37, PLCF19, PLCF7 and PLCF1.

4. Conclusions

Modes distribution and confinement losses in photonic crystal fibers with different solid cores infiltrated with a liquid crystal were analyzed. The experimental results obtained confirm the influence of a core diameter on light propagation. It appeared that the size of the core does not only increases the number of modes, but also decreases attenuation predominantly due to the scattering on an infiltrated liquid crystal. The main conclusion from the analysis is that the measured attenuation is much larger than confinement losses, so it can suggest that the material losses are predominant. Moreover the measured losses were strongly correlated with the amount of optical power guided through the area filled with a liquid crystal. This explains why the measured losses of the PLCF with the largest core were the lowest even if the calculated confinement losses were much higher than for other PLCFs considered. Photonic liquid crystal fibers with a large core and small attenuation can be used in sensors based on all-in-fiber components. Also they can be used in optical filters, where low attenuation is needed, e.g. in a tunable filter based on two cascaded photonic liquid crystal fibers

[36] where the position and bandwidth of guided waves can be controlled.

Acknowledgements

This work was partially supported by the National Centre For Research and Development under the grant no. LIDER/05/208/L-3/11/NCBR/2012. A fruitful collaboration with Prof. Roman Dąbrowski (Military University of Technology, Warsaw, Poland) is gratefully acknowledged.

References

[1] P. St. J. Russell, Photonic-Crystal Fibers, J. Lightwave Technol 24 (12) (2006) (4729–4749).
[2] T.P. White, R.C. McPhedran, C. Martijnde Sterke, N.M. Litchinitser, B.J. Eggleton, Resonance and scattering in microstructured optical fibers, Opt. Lett. 27 (22) (2002) 1977–1979.
[3] J. Laegsgaard, Gap formation and guided modes in photonic bandgap fibres with high-index rods, J. Opt. A–Pure Appl. Opt. 6 (8) (2004) 798–804.
[4] S. Ertman, A.H. Rodriguez, M.M. Tefelska, M.S. Chychlowski, D. Pysz, R. Buczynski, E. Nowinowski-Kruszelnicki, R. Dabrowski, T.R. Wolinski, Index guiding photonic liquid crystal fibers for practical applications, J. Lightwave Technol. 30 (8) (2012) 1208–1214.
[5] S. Février, R. Jamier, J.-M. Blondy, S.L. Semjonov, M.E. Likhachev, M.M. Bubnov, E.M. Dianov, V.F. Khopin, M.Y. Salganskii, A.N. Guryanov, Low-loss single mode large mode area all-silica photonic bandgap fiber, Opt. Express 14 (2) (2006) 562–569.
[6] A. Lorenz, H.-S. Kitzerow, A. Schwuchow, J. Kobelke, H. Bartelt, Photonic crystal fiber with a dual-frequency addressable liquid crystal: behavior in the visible wavelength range, Opt. Express 16 (23) (2008) 19375–19381.
[7] T.T. Alkeskjold, A. Bjarklev, Electrically controlled broadband liquid crystal photonic bandgap fiber polarimeter, Opt. Lett. 32 (12) (2007) 1707–1709.
[8] M.M. Tefelska, T.R. Woliński, S. Ertman, K. Mileńko, R. Łączkowski, A. Siarkowska, A.W. Domański, Electric field sensors based on micro-electrodes systems with photonic liquid crystal fibers, J. Lightwave Technol. 33 (12) (2014) 1–7.
[9] W.-H. Ding, Y. Jiang, Miniature photonic crystal fiber sensor for high-temperature measurement, IEEE Sens. J. 14 (3) (2014) 786–789.
[10] S. Ertman, P. Lesiak, T. Woliński, Optofluidic photonic crystal fiber-based sensors, J. Lightwave Technol. PP (99) (2016) 1.
[11] J. Villatoro, J. Zubia, New perspectives in photonic crystal fibre sensors, Opt. Laser Technol. 78 (A) (2016) 67–75.
[12] Iam-Choon Khoo, Liquid Crystals, second edition, John Wiley & Sons, 2007, 2017.
[13] M. Murawski, L.R. Jaroszewicz, K. Stasiewicz, A photonic crystal fiber splice with a standard single mode fiber, Photon. Lett. Poland 1 (3) (2009) 115–117.
[14] M. Nielsen, C. Jacobsen, N. Mortensen, J. Folkenberg, H. Simonsen, Low-loss photonic crystal fibers for transmission systems and their dispersion properties, Opt. Express 12 (7) (2004) 1372–1376.
[15] K. Tajima, J. Zhou, K. Nakajima, K. Sato, Ultralow loss and long length photonic crystal fiber, J. Lightwave Technol. 22 (1) (2004) (7).
[16] J.A. Sánchez-Martín, M. Ángel Rebolledo, J. Miguel Álvarez, J.A. Vallés, A. Díez, M.V. Andrés, Erbium-doped-silica photonic crystal fiber characterization method: description and experimental check, IEEE J. Quantum Electron. 46 (8) (2010) 1145–1152.
[17] W. Chen, S. Li, P. Lu, Erbium-doped photonic crystal fiber: fabrication and its gaining characteristics, Lasers & Electro Optics & The Pacific Rim Conference on Lasers and Electro-Optics (2009) 1–2.
[18] T.R. Woliński, A. Czapla, S. Ertman, M. Tefelska, A.W. Domański, E. Nowinowski-Kruszelnicki, R. Dąbrowski, Tunable highly birefringent solid-core photonic liquid crystal fibers, Opt. Quantum Electron. 39 (2007) 1021–1032.
[19] L. Wei, T. Alkeskjold, A. Bjarklev, Tunable and rotatable polarization controller using photonic crystal fiber filled with liquid crystal, Appl. Phys. Lett. 96 (24) (2010) (241104-241104-3).
[20] L. Scolari, T.T. Alkeskjold, J. Riishede, A. Bjarklev, D.S. Hermann, M. Anawati, D. Nielsen, P. Bassi, Continuously tunable devices based on electrical control of dual-frequency liquid crystal filled photonic bandgap fibers, Opt. Express 13 (19) (2005) 7483–7496.
[21] B.T. Kuhlmey, B.J. Eggleton, D.K.C. Wu, Fluid-filled solid-core photonic bandgap fibers, J. Lightwave Technol. 27 (11) (2009).
[22] A. Lorenz, R. Schuhmann, H.-S. Kitzerow, Switchable waveguiding in two liquid crystal-filled photonic crystal fibers, Appl. Opt. 49 (2010) 3846–3853, http://dx.doi.org/10.1364/AO.49.003846.
[23] A. Lorenz, R. Schuhmann, H.-S. Kitzerow, Infiltrated photonic crystal fiber: experiments and liquid crystal scattering model, Opt. Express 18 (2010) 3519–3530, http://dx.doi.org/10.1364/OE.18.003519.
[24] A. Lorenz, H.-S. Kitzerow, Efficient electro-optic switching in a photonic liquid crystal fiber, Appl. Phys. Lett. 98 (2011) 241106, http://dx.doi.org/10.1063/1.3599848.
[25] M. Wahle, J. Ebel, D. Wilkes, H.-S. Kitzerow, Asymmetric band gap shift in electrically addressed blue phase photonic crystal fibers, Opt. Express 24 (20) (2016) 22718–22729, http://dx.doi.org/10.1364/OE.22.000262.
[26] M. Wahle, H.-S. Kitzerow, Electrically tunable zero dispersion wavelengths in photonic crystal fibers filled with a dual frequency addressable liquid crystal, Appl. Phys. Lett. 107 (2015) 201114, http://dx.doi.org/10.1063/1.4936086.
[27] M. Wahle, H.-S. Kitzerow, Measurement of group velocity dispersion in a solid-core photonic crystal fiber filled with a nematic liquid crystal, Opt. Lett. 39 (16) (2014) 4816–4819, http://dx.doi.org/10.1364/ol.39.004816.
[28] M.M. Tefelska, S. Ertman, T.R. Wolinski, P. Mergo, R. Dabrowski, Large area multimode photonic band-gap propagation in photonic liquid-crystal fiber, IEEE Photon. Technol. Lett. 24 (8) (2012) 631–633.
[29] COMSOL 3.5a, Comsol Multiphysics [Online], 2017, Available at: http://www.comsol.com.
[30] S. Ertman, T.R. Wolinski, J. Beeckman, K. Neyts, P.J.M. Vanbrabant, R. James, F.A. Fernández, Numerical simulations of electrically induced birefringence in photonic liquid crystal fibers, Acta Phys. Pol. A 118 (6) (2010) 1113–1117.
[31] R. Dabrowski, J. Dziaduszek, Z. Stolarz, J. Kedzierski, Liquid crystalline materials with low ordinary index, J. Opt. Technol. 72 (9) (2005) 662–667.
[32] R. Dabrowski, New liquid crystalline materials for photonic applications, Mol. Cryst. Liq. Cryst. 421 (1) (2005) 1–21.
[33] I.H. Malitson, Interspecimen comparison of the refractive index of fused silica, J. Opt. Soc. Am. 55 (10) (1965) 1205.
[34] A. Hochman, Y. Leviatan, Calculation of confinement losses in photonic crystal fibers by use of a source-model technique, J. Opt. Soc. Am. B 22 (2005) 474–480.
[35] M.M. Tefelska, S. Ertman, T. Wolinski, P. Mergo, R. Dabrowski, Attenuation of the photonic liquid crystal fibers with various core diameters, Proc. SPIE 8794 (2013) 879429.
[36] M.M. Tefelska, Sławomir Ertman, Tomasz R. Woliński, Roman Dąbrowski, Paweł Mergo, Tunable filter based on two cascaded photonic liquid crystal fibers, Photon. Lett. Poland 5 (1) (2013) 14–16.